



# Dual thermal ecotypes coexist within a nearly genetically identical population of the unicellular marine cyanobacterium Synechococcus

Joshua D. Kling<sup>a</sup> 📵, Michael D. Lee<sup>b,c</sup> 📵, Nathan G. Walworth<sup>a</sup>, Eric A. Webb<sup>a</sup> 📵, Jordan T. Coelho<sup>a</sup> 📵, Paul Wilburn<sup>b,d</sup>, Stephanie I. Anderson<sup>e,f</sup> 📵, Qiangian Zhou<sup>g</sup>, Chunguang Wang<sup>g</sup>, Megan D. Phan<sup>a</sup>, Feixue Fu<sup>a</sup>, Colin T. Kremer<sup>d,h</sup>, Elena Litchman<sup>d,i</sup>, Tatiana A. Rynearson<sup>e</sup>, and David A. Hutchins<sup>a,1</sup>

Edited by Simon Levin, Princeton University, Princeton, NJ; received September 14, 2023; accepted October 11, 2023

The extent and ecological significance of intraspecific functional diversity within marine microbial populations is still poorly understood, and it remains unclear if such strain-level microdiversity will affect fitness and persistence in a rapidly changing ocean environment. In this study, we cultured 11 sympatric strains of the ubiquitous marine picocyanobacterium Synechococcus isolated from a Narragansett Bay (RI) phytoplankton community thermal selection experiment. Thermal performance curves revealed selection at cool and warm temperatures had subdivided the initial population into thermotypes with pronounced differences in maximum growth temperatures. Curiously, the genomes of all 11 isolates were almost identical (average nucleotide identities of >99.99%, with >99% of the genome aligning) and no differences in gene content or single nucleotide variants were associated with either cool or warm temperature phenotypes. Despite a very high level of genomic similarity, sequenced epigenomes for two strains showed differences in methylation on genes associated with photosynthesis. These corresponded to measured differences in photophysiology, suggesting a potential pathway for future mechanistic research into thermal microdiversity. Our study demonstrates that present-day marine microbial populations can harbor cryptic but environmentally relevant thermotypes which may increase their resilience to future rising temperatures.

Synechococcus | temperature adaptation | intraspecific diversity | epigenomics

Marine bacteria control most marine biogeochemical cycles (1, 2) and are composed of an estimated  $10^{10}$  species (3). In addition, bacterial species complexes include numerous strains or ecotypes (4-8). Much of the work documenting the ecological relevance of intraspecific microdiversity has used amplified marker genes such as the 16S rRNA gene (9), and little has been done to describe the genotypic and (more importantly) phenotypic diversity within groups that are identical at the 16S rRNA level. At higher taxonomic levels, microbial interspecific diversity has a recognized role of increasing the stability of biogeochemical cycling and resilience to a changing environment (10). In order to understand the ability of microbial populations to persist and maintain their functional roles under changing thermal regimes, it is also important to assess the diversity of thermal responses that exists within microbial populations (11–13).

Efforts to understand the interactions of microbes with their environment have often relied on approaches that underestimate or mask intraspecific diversity. For instance, culture-based methods are often limited to a handful of strains that are amenable to cultivation or are currently available in culture collections. These are then used to make generalizations about the activity of a broader taxonomic group (14-16). Sequencing approaches avoid this culturing bottleneck but lack the ability to provide rate measurements. Furthermore, metagenomic or metatranscriptomic analysis pipelines often are unable to discern sequencing errors from rare genotypes or strains (17). In addition, purely sequence-based in situ approaches are also limited in the amount of ecotypic microdiversity they can reveal, simply because detection relies on observed correlations between relative abundance and ambient environmental parameters (e.g., temperature, nutrients, and light). Thus, rare ecotypes with optimal niches that lie outside of current conditions will remain cryptic unless the environment changes. For example, most marine microbial communities will undergo future selection by temperatures exceeding those that they currently experience (18, 19), as current climate models predict that anthropogenic carbon emissions will raise sea surface temperatures (SST) ~4 °C by the year 2100 (20).

Marine unicellular picocyanobacteria are particularly important to our understanding of how biogeochemical cycling will change with rising SST. The genus Synechococcus is a major microbial functional and taxonomic group that is found from the equator to high

## **Significance**

Numerous studies exist comparing the responses of distinct taxonomic groups of marine microbes to a warming ocean (interspecific thermal diversity). For example, Synechococcus, a nearly globally distributed unicellular marine picocyanobacterium that makes significant contributions to oceanic primary productivity, contains numerous taxonomically distinct lineages with well-documented temperature relationships. However, little is known about the diversity of functional responses to temperature within a given population where genetic similarity is high (intraspecific thermal diversity). This study suggests that considerable unrecognized thermal microdiversity exists in current marine Synechococcus populations, which could help this biogeochemically essential microbial group adapt to a warmer ocean.

The authors declare no competing interest.

This article is a PNAS Direct Submission.

Copyright © 2023 the Author(s). Published by PNAS. This article is distributed under Creative Commons Attribution-NonCommercial-NoDerivatives License 4.0

<sup>1</sup>To whom correspondence may be addressed. Email: dahutch@usc.edu.

This article contains supporting information online at https://www.pnas.org/lookup/suppl/doi:10.1073/pnas. 2315701120/-/DCSupplemental.

Published November 16, 2023.

polar latitudes (8, 21). This diverse genus is responsible for an estimated 16.7% of marine primary production and is expected to increase in both abundance and distribution as a result of warming (22, 23). It has also been strongly correlated with carbon export to the deep ocean (24), making it an important component of the marine carbon cycle.

In this study, we used multiple temperature incubations of a natural coastal assemblage to enrich for "thermal specialist" strains of *Synechococcus*. We then isolated multiple sympatric strains from the contrasting temperature incubations and characterized their thermal niches, allowing us to recover two co-occurring but distinct thermal phenotypes (cool and warm) from a single initial water sample. Finally, we sequenced and assembled high-quality draft genomes for all the isolates. Upon comparing their assemblies, the two sets of thermally distinct isolates are nearly identical, with an average nucleotide identity (ANI) >99.99%. We additionally could not detect any genetic variation that differentiated both thermotypes. Analysis of the epigenome for one cool- and warm-temperature isolate leads us to hypothesize that methylation could potentially contribute to the thermal specializations observed in this population.

#### **Results**

**Thermal Phenotype.** Out of the 11 strains of *Synechococcus* examined, one was isolated from 22 °C Narragansett Bay seawater within hours of collection (*SI Appendix*, Table S1). The other ten were collected after 2-wk enrichment experiments using the same seawater, five each from the 18 °C and 30 °C treatments, all of which shared identical morphologies (*SI Appendix*, Table S1). Because the 22 °C in situ conditions and 18 °C experimental treatment represent temperatures that currently occur in Narragansett Bay, these isolates are considered together and are referred to as "cool-temperature isolates." We compared these against "warm-temperature isolates" collected from the 30 °C incubations, a temperature exceeding those currently recorded at our time series collection site (https://web.uri.edu/gso/research/plankton/data/).

We generated Thermal Performance Curves (TPC) for each isolate after growing them across multiple temperatures (average  $R^2$  = 0.81; ±0.14 SD; Fig. 1*A* and *SI Appendix*, Fig. S1 and Table S2). Average thermal maximum (Tmax) was higher for warm (35.6 °C, ±0.5 SD) compared to cool-temperature isolates (33.5 °C, ±0.9; t test, P = 0.005; Fig. 1*B* and Table 1). Optimal growth temperatures (Topt) were also higher for isolates from warm (average = 29.8 °C, ±1.8 SD) than cool-temperature isolates (27.6 °C, ±1.2 SD); however, this difference was not statistically significant (P = 0.06).

Minimum growth temperature (Tmin) and niche width (Tmax–Tmin) did not significantly differ between groups (P = 0.91).

In addition to differences in growth observed using in vivo fluorescence, we compared the warm-temperature isolate LA127 (Topt = 29.7 °C, Tmax = 35.3 °C) and the cool-temperature isolate LA31 (Topt = 27.1 °C, Tmax = 31.7 °C) when the temperature was increased from 22 to 28 °C, closer to their Topt (*SI Appendix*, Table S2). This showed that at higher temperature, the warm-temperature isolate accumulated ~2× more volume-normalized particulate organic carbon (POC; P = 0.002), while the cool-temperature isolate LA31 ceased growing by day 2 (*SI Appendix*, Fig. S2A). Because LA31 quickly entered the stationary phase at 28 °C, the warm-temperature isolate maintained a higher, but not statistically significant (P = 0.07), growth rate as calculated across all 4 d (*SI Appendix*, Fig. S2B).

**Comparative Genomics.** To compare genomic differences between cool and warm isolates, sequence data were assembled into a 100% complete genome for each isolate (n = 11) (*SI Appendix*, Table S3). On average, assemblies were 2.74 Mbp long (±0.007 SD), split between an average of 21 (±1 SD) contigs with a mean GC content of 63% (±0.00) and mean gene count of 2978.0 (±11 SD). Average nucleotide identity (ANI) between these draft genomes showed that they were on average 99.9964% identical (±0.003 SD) across >99% of the assembly (*SI Appendix*, Fig. S2). For comparison, the average ANI between all isolates from this study and the next closest relative on NCBI (strain CB0101, from the nearby Chesapeake Bay) was 85.46% ANI.

To examine genomic variation among these isolates with high ANI, draft genomes were aligned to the closed *Synechococcus* reference genome (25) using parsnp to detect single nucleotide polymorphisms (SNPs). A total of 24 SNP sites were detected across all 11 assemblies. Constructing a phylogenetic tree using these SNP sites did not segregate isolates into cool and warm temperature phenotypes (Fig. 2*A*) and neither did this alignment-based approach highlight major genomic rearrangements (Fig. 2*B*). A 110-kb region was excluded from the SNP-based analysis which suggested either poor alignment due to breaks in short-read assemblies, or a highly variable accessory genome.

To explore the possibility of a highly variable accessory genome related to this 110-kb gap in the parsnp analysis, assemblies were compared with the Anvi'o pangenomic pipeline. Out of 2,985 gene clusters that were identified, (*SI Appendix*, Fig. S4 and Table S4) 33 had either functional (e.g. differences in sequence) or structural (e.g. insertions, deletions) differences; however, no genomic differences were found in these clusters that correlated with strain

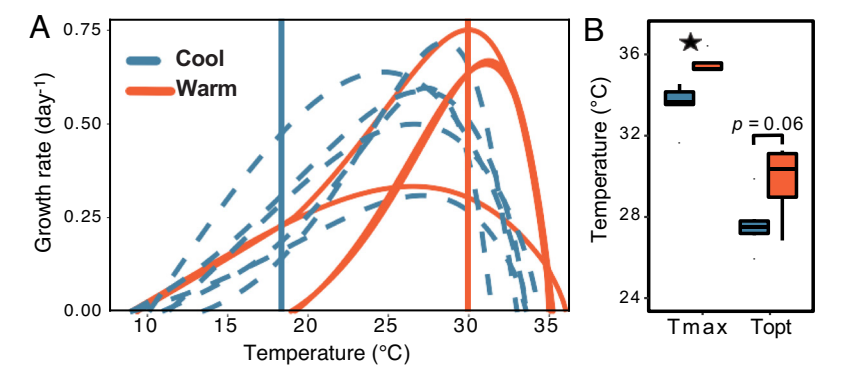


**Fig. 1.** Thermal growth rate responses of *Synechococcus* isolates examined in this study, depending on whether the isolate came from cool (blue; 18 to 22 °C) or warm (red; 30 °C) incubation experimental temperatures. (*A*) TPC for all isolates determined using the Eppley–Norberg approach. Vertical lines indicate 18 °C (blue) and 30 °C (red). (*B*) Boxplots showing the maximum temperature limit (Tmax) and optimal temperature (Topt) for the two sets of isolates. Error bars represent quartiles, and the star indicates P < 0.05 level (t test).

Table 1. Thermal performance curve parameters (TPC, C°) for 11 *Synechococcus* isolates, including Tmax (Thermal maximum), Tmin (Thermal minimum), Topt (Thermal optimum), and total TPC Width; n is the number of isolates tested from each incubation temperature

Temperature (n)		Parameter	Mean	SD	Max	Min
22° Initial	(1)	Tmax	33.8			
		Topt	27.9			
		Tmin	11.2			
		Width	21.8			
18°	(5)	Tmax	33.4	1.0	34.3	31.7
		Topt	27.6	1.4	29.8	26
		Tmin	12.4	3.1	14.8	9.0
		Width	21.0	2.5	24.5	18.9
30°	(5)	Tmax	35.6	0.5	36.5	35.3
		Topt	29.8	1.8	31.3	26.8
		Tmin	14.2	4.4	19.1	9.0
		Width	21.4	4.7	26.3	16.1

isolation temperature or measured TPC (*SI Appendix*, Fig. S4). All detected differences were places the contigs broke in any of the 11 assemblies, which explains the region excluded from parsnp. Finally, we were able to close an additional genome, allowing us to do a whole genome alignment between the reference genome (cool-temperature isolate LA31: Topt = 27.5 °C, Tmax = 31.7 °C) and a warm-temperature isolate (LA127: Topt = 29.7 °C, Tmax = 35.3 °C). No genomic rearrangements were detected between isolates (*SI Appendix*, Fig. S5) and the predicted number of SNPs (n = 21) was similar to the output from parsnp for all draft genomes (n = 24). Finally, we screened for potential interactive effects with associated bacteria, but found no link to thermal performance (*SI Appendix*, Fig. S6).

**Epigenomics.** We also compared cytosine methylation between LA31 (cool isolate) and LA127 (warm isolate) using Oxford Nanopore sequences. LA31 had 1,202 methylated cytosines across its genome with 1,062 (88%) located in coding regions. LA127 had 1,073 methylated cytosines with 957 (89%) located in coding regions. As a check of possible methylation in promoter regions, we looked for methylated C's within 35 bp of coding start sites; however, none were observed in either strain (Dataset S1). The genomes shared 436 methylation sites, with the majority being unique to each strain. However, the methylated genes belonged to similar KEGG modules (*SI Appendix*, Fig. S7). The

genome assemblies for every isolate had 42 genes annotated as methyltransferases using the KEGG database.

Notably, we detected methylation in coding regions for two phycobilisome linker proteins (Fig. 3*C*) only in the warm-temperature isolate. These genes were not methylated in the cool-temperature isolate; however, in this isolate one of the two copies of the phycocyanin beta chain did contain a methylated cytosine. The cool-temperature isolate was also methylated in a single gene coding for *atpH* (ATPase subunit delta, *SI Appendix*, Table S6) while the warm-temperature isolate had two different methylated ATPase subunits (gamma and beta) as well as a subunit of photosystem I (*psaD*) and a component of the cytochrome b6-f complex (*petA*) (*SI Appendix*, Table S7).

The null model analysis of genome methylation enrichment for both LA127 and LA31 genomes suggested that methylation is concentrated in coding regions for both strains (P < 0.001), consistent with prior observations of methylated sites enriched in gene regions in other cyanobacteria (26). Likewise, in both LA127 and LA31, methylation overlapped with photosystem-related genes more often than by chance alone (P < 0.05), suggesting that methylation plays a role in photosystem metabolism in both strains. However, as expected, the difference in the uniquely methylated photosystemrelated genes between LA127 (n = 2; SI Appendix, Table S7) and LA31 (n = 5; SI Appendix, Table S6) was not sufficient to yield significant differences in the total level of enrichment of photosystem-related methylation in each genome. While the null model analyses of these several photosystem genes did not suggest significantly enriched methylation from sampling of only these two epigenomes, we note that the full complement of photosystem-related genetic elements tested here may not be exhaustive due to limitations in annotation. Further research with more cold- and warm-adapted epigenomes is needed to robustly determine whether significant differences exist in photosystem methylation patterns between the two thermotypes. It is also well-documented that single molecular changes can cause adaptive phenotypic differences in microbial taxa (27–29) irrespective of enrichment, which we cannot rule out here in view of the <100 bp that varied between the two genomes. Nevertheless, the fact that we observed only a handful of differences in methylation within photosystem-related genes relative to deep conservation of all other genomic and epigenomic sites paves the way for more targeted studies examining the impact of these genes on temperature-related phenotypes in *Synechococcus*.

**Photophysiology.** Although no genomic variation was detected between our two closed genomes at loci associated with C-phycocyanin, photosystem I, or photosystem II, both strains had measurably different photophysiology and similarly showed

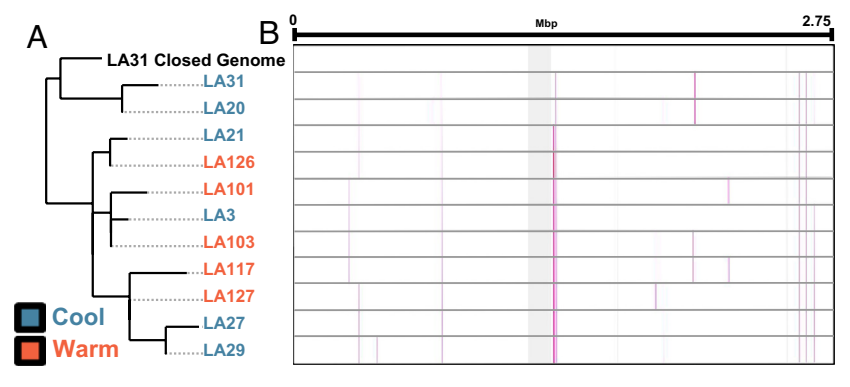


**Fig. 2.** Alignment to detect SNPs in portions of the genome present in all draft genomes and the reference. (*A*) A total of 24 SNPs were detected in the core genome and used to construct a phylogenetic tree. The locations of each of these SNP sites (purple vertical lines) are shown in (*B*). Genomic rearrangements in any of the draft genomes would also be highlighted in (*B*) if they were present.

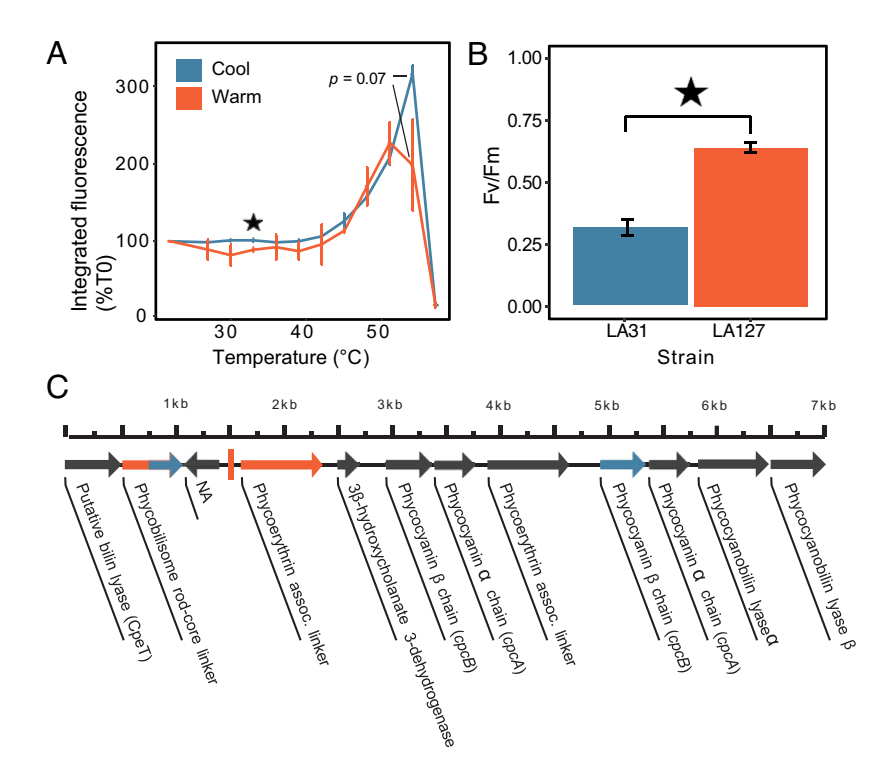


**Fig. 3.** (*A*) Mean whole-cell integrated fluorescence (600 to 700 nm) with temperature for warm and cool strains and (*B*) Photochemical efficiency ( $F_v/F_m$ ) of PSII at 28 °C and an excitation wavelength matching phycocyanin and allophycocyanin (645 nm). The star indicates observations that were statistically different (*t* test, P < 0.05), and error bars represent ±1 SD from triplicate trials. (*C*) The locus containing genes coding for C-phycocyanin biosynthesis. Methylated coding regions are colored based on which isolate they were detected in and a colored vertical line is used to show methylation detected outside of any coding regions. Blue colors indicate the cool temperature (18 to 22 °C) isolate LA31, while red shows warm temperature (30 °C) isolate LA127. Coding regions that were methylated for both cool and warm strains contain both colors. Gene function as determined by Kegg Ortholog (KO) ID is shown. Coding regions that were not assigned a KO ID are labeled as "NA."

differences in methylation within loci coding for these systems (Fig. 3 and SI Appendix, Tables S5–S7). We estimated photosystem thermal tolerance in both strains using whole-cell fluorescence spectra matching the accessory pigment C-phycocyanin. Fluorescence levels were measured starting at 22 °C and while slowly ramping up to 57 °C, as an indicator of loss of photosynthetic function due to heat stress (Fig. 3A). Fluorescence for both isolates increased exponentially between 48 and 54 °C, indicating light-harvesting energetic losses to fluorescence increase as the photosynthetic antenna complex becomes stressed by warming temperatures and then abruptly crashed to zero at 57 °C as the antenna complex dissociated completely. At physiologically relevant temperatures below 45 °C (t test, P = 0.05) and at the 54 °C fluorescence peak (t test, P = 0.07), the warmtemperature isolate had lower fluorescence, suggesting that it is better able to maintain its functionality under extreme thermal stress than the cool-temperature isolate.

Furthermore, both isolates had differing photophysiologies when comparing warming effects on the key photosynthetic efficiency parameter  $F_v/F_m$  (Fig. 3*B*). When acclimated to 28 °C, photosystem II efficiency in the warm-temperature isolate was more than twice as high as in the cool-temperature isolate (*t* test,  $P = 1.04 \times 10^{-7}$ ). The values reported here are analogous to  $F_v/F_m$  measurements reported for other marine *Synechococcus* spp. (30).

### **Discussion**

This study demonstrates the coexistence of distinct but cryptic thermal phenotypes within a single population of coastal *Synechococcus*. Although previous work has established that distinct functionally relevant ecotypes can coexist within populations of picocyanobacteria (e.g., refs. 7 and 31), we found evidence for pronounced thermal trait diversity among nearly identical clonal strains within a

population. Thermal selection of a natural population at either 18 °C or 30 °C revealed the presence of cool and warm thermotypes with distinct thermal response curves and photophysiology. Remarkably, the genomes of both cool and warm thermotypes were nearly identical (>99.99% ANI) despite their different thermal characteristics.

Examining gene and SNP content across the high-quality genomes for these thermotypes did not reveal a DNA-based mechanism that explained their phenotypic differences. We did detect a pattern of cytosine methylation within genes coding for C-phycocyanin (a component of the light-harvesting machinery) that differed between a warm- and cool-temperature isolates. Although we could not statistically rule out random occurrence of this methylation enrichment using only two samples, this methylation pattern was the only parameter we observed that corresponded to significant differences in both thermal resilience of the phycobilisome accessory pigment complex and overall photosynthetic efficiency ( $F_{\rm v}/F_{\rm m}$ ).

Previous literature has suggested a strong connection between variation among genes encoding the photosynthetic machinery and thermal adaptation in marine *Synechococcus* (30). Variation in orthologous photosystem genes at the DNA level is well supported in marine *Synechococcus* as a key mechanism for the broad distribution of this genus across temperature regimes (32, 33). In *Synechococcus* subcluster 5.3, variation in R-phycocyanin strongly correlated with *Synechococcus* thermal adaptation (26). R-phycocyanin is an ortholog of the C-phycocyanin where we detected epigenetic variation between the thermotypes examined here. It has also been shown that at elevated temperatures a tropical, low-latitude *Synechococcus* strain had lower fluorescence of the antenna pigment complex (indicating more efficient photosynthetic energy capture) than a subpolar strain, similar to the trend we observed between warm

and cool temperature phenotypes in our study, and that intracellular concentrations of phycobilisome proteins increase under high temperatures (30, 34).

Although our experimental design precludes looking at the relative abundance of each ecotype in the original population, we note that the one isolate collected directly from the environment was the cool temperature ecotype. The average summertime surface water temperature at our sample site for the period from 1957 to 2019 was 20.6 °C, with a maximum of 26.5 °C (Fig. 4A). This distribution of temperatures falls below the Topt for both ecotypes, but will favor the cool temperature thermotypes. The higher growth rates of cool-temperature isolates under typical summer conditions suggest that having the warm temperature phenotype has a fitness cost (when defined purely by growth rates), and the shape of thermal curves suggests that the warm temperature phenotype only has a growth advantage above the maximum daily high temperature observed (26.5 °C). In theory, selection (considering only growth rates) should remove this phenotype from the population (35 and references therein).

It is possible that the warm-temperature thermotypes could represent an adaptation to a heterogeneous shallow coastal ecosystem. Tidal movements within Narragansett Bay may periodically move this population farther into the estuary where temperatures in shallow coves in Narragansett Bay can exceed 30 °C (36), favoring the warm temperature thermotypes. Another possible explanation for this thermal diversity is that these microbes originated in warmer low latitude waters and were advected into this relatively cooler region as part of the northerly flow of the nearby Gulf Stream. It has been estimated that microbes entrained in the Gulf Stream may experience a range of temperatures as a result of latitudinal advection that is larger than changes due to seasonal patterns (37). Wind-driven circulation during summer months facilitates persistent exchange between estuarine waters in the Bay and oceanic waters in Rhode Island Sound, and allochthonous inputs of subtropical phytoplankton are possible (38-40) and supported by the recurring appearance of subtropical fish species in Narragansett Bay (41).

The presence of a warm temperature thermotype could be a source of preadaptations to the warmer conditions that are expected in the future. In Narragansett Bay, average summer SST has been increasing at a rate of 0.03 °C per year since 1957 (Fig. 4A), meaning that the average summertime SST will likely increase to ~23 °C by the end of the century. Assuming a similar distribution of temperatures in the year 2100, there will be periods when SST is above the average Topt of the low-temperature ecotype, and

conditions will favor the high-temperature ecotype (Fig. 4*B*). Any continued trend of rising temperatures beyond 2100 will continue to further expand the niche of the warm temperature ecotype.

These coexisting thermotypes are also interesting in the context of marine *Synechococcus* evolution, as temperature is thought to be a key driver of diversity between clades within this group (8, 32). It is possible that intraspecific microdiversity of thermal phenotypes could have been a contributing mechanism in the diversification of *Synechococcus* into the distinct lineages observed today. When a population consisting of multiple thermotypes encounters a novel thermal environment, one phenotype may be selected over another, potentially leading to genetic divergence and speciation. Further studies will be needed on intraspecific microdiversity between nearly identical strains, to assess its potential role in the evolution of *Synechococcus* and microbes in general.

Our findings also have implications for our general understanding of biological responses to rising temperatures. In the context of ocean acidification, previous studies have shown a higher diversity of responses between phytoplankton ecotypes within a taxonomic group than between them (15, 42). Our study takes this further by showing that distinct responses to climate impacts can coexist even within a nearly genetically identical population. This microdiversity in thermal traits also has been detected in other marine phytoplankton. In a similar study conducted within Narragansett Bay, TPC of recently isolated strains of the diatom genus Skeletonema were compared and showed a similar high degree of intraspecific diversity of thermal traits (43). This previous study also observed a similar significant difference in thermal maxima (Tmax) across strains and suggested that variability at such thermal limits plays an important role in both ecological and biogeochemical dynamics. Because of the high degree of genetic similarity between these isolates, standard amplicon sequencing or metagenomic microbial surveys would not be able to detect this level of functional microdiversity.

Our results show that ecologically important thermal niche variability in *Synechococcus* is sometimes not related to discernible genomic differences, and raises the question of whether the epigenome may play a role in this trait. Further work will be needed, however, to mechanistically link the N-5 cytosine methylation of phycocyanin genes we observed to correlated differences in thermal niche and photophysiology. Evidence from the related model cyanobacterium *Synechocystis* shows that N-4 cytosine methylation can sometimes regulate photosynthetic gene expression. Mutation of the gene for a DNA methyltransferase involved in this reaction results

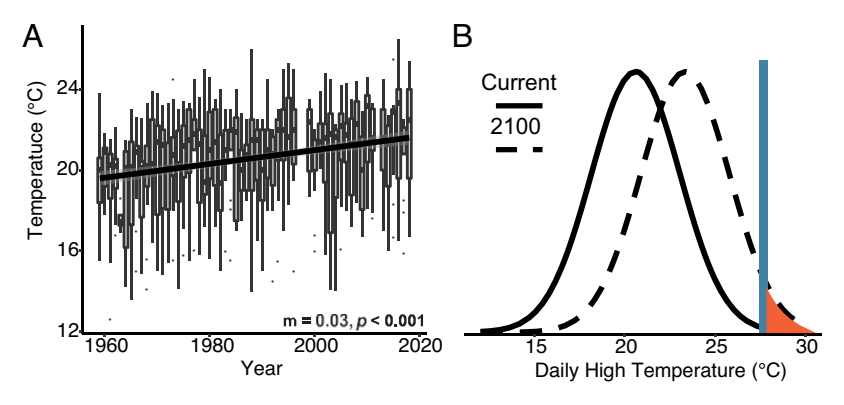


**Fig. 4.** (*A*) Boxplot of summertime (June to August) sea surface temperature (SST) increases at the Narragansett Bay Time Series from 1957 to 2019 (https://web.uri.edu/gso/research/plankton/data/). Trendline shows the output of a linear model fit to the data. The slope of this model and the *P* value are shown below the data. (*B*) Hypothetical normal seasonal temperature distributions created using the mean of the recent data shown in panel *A* (solid line), and the predicted distribution of these data in the year 2100 (dashed line) using the slope of the linear model. A blue vertical line shows the average Topt for all cool-temperature isolates. Temperatures above this line, which will likely favor warm temperature ecotypes, are shown in red.

in changes in cellular photophysiology and phycocyanin-to-chlorophyll ratios (44, 45). In fact, cytosine or adenine methylation can regulate transcription in many bacteria, as well as influencing DNA replication and repair, virulence, and viral defense (46, 47). Vascular plants employ cytosine methylation to generate phenotypic plasticity in response to a variety of environmental stressors (48); for instance, thermal stress results in extensive changes in genome methylation of the marine seagrass *Posidonia* (49). Epigenetics is thought to be an especially important source of phenotypic variability in plants that reproduce clonally (50), as do cyanobacteria and most other marine microbes. Advances in technology such as SMRT (single molecule real-time) sequencing offer the ability to detect multiple modes of DNA methylation, including C5-methyl-cytosine, N4-methylcytosine, and N6-methyl-adenine (51, 52). Our nanopore-based long-read methodology detected only C5-methylcytosine, so it is possible that the other two types of methylation not measured here could have contributed to the observed thermal phenotypes.

It is evident that understanding thermal microdiversity may sometimes require delving much deeper into molecular mechanisms than is typical in most metagenomic studies. In the case of our estuarine Synechococcus, this cryptic thermal microdiversity will likely contribute to this population's ability to continue occupying its picoplanktonic niche, even in the face of considerable increases in environmental temperatures. Another important implication is that culture studies using a single isolate or strain from a population grown briefly under a limited set of environmental conditions may underestimate that population's resilience to warming. A better understanding of the existing functional thermal microdiversity within populations is needed to accurately model the impact that future elevated temperatures will have on microbial communities and on the biogeochemical cycles that they regulate.

#### **Materials and Methods**

Sampling and Cell Isolation. All strains were isolated from the Narragansett Bay Time Series site (latitude 41.47, longitude -71.40) on July 18th, 2017 (39). Full methods can be found in ref. 25. In short, sample water was prefiltered (200 µm mesh) to remove large grazers and detritus and enriched using F/40 medium (53) under four temperatures [18°, 22° (control), 26°, and 30 °C] in triplicate 2L polycarbonate bottles. All culturing in this study was done with a 12:12 light-dark cycle at 150 µmoles photons m<sup>-2</sup> s<sup>-1</sup>. Enrichments were diluted semicontinuously with a sterile medium to avoid cells entering the stationary phase. At the time of collection and after 10 d of enrichment, individual cells with measurable phycocyanin fluorescence were sorted into 96-well plates using a BD Influx using single-cell sorting mode. Isolated clonal strains were maintained long-term in F/2 (53) made with artificial seawater (54) at 22 °C in 1 L bottles (with ~20% headspace and daily shaking to suspend the cells and facilitate gas exchange), with weekly transfers.

Thermal Performance Assays. TPC were measured for 11 strains isolated from initial surface seawater (n = 1),  $18^{\circ}$  (n = 5), and  $30^{\circ}$ C (n = 5) (Table 1). Cultures were temperature acclimated (with dilution) in triplicate 8 mL borosilicate vials containing 5 mL of F/2 medium from 9 to 33 °C for 2 wk. Higher temperatures were added for isolates able to grow at 33 °C. This temperature range was chosen because it exceeds current summertime conditions in Narragansett Bay (55) but encompasses projected SST increases (20). Biomass was recorded every two days using in vivo chlorophyll a fluorescence measured on a Turner AU 10 fluorometer (Turner Designs Inc.), and growth rates and Eppley-Norberg TPC (56) were calculated in R (57) using the package growthTools (DOI: 10.5281/zenodo.3634918). Cultures were screened for algal contaminants using fluorescence microscopy. In strains LA20 and LA27, no cells were observed after 2 wk of acclimation at 9 °C, so the growth rate was set to zero. Maximum growth rates were not necessarily comparable between different thermal curve experiments, due to minor differences in growth stage at the time of sampling.

Elemental Stoichiometry, Carbon Fixation, and Photophysiology. We verified differences in thermal phenotype for two strains, LA31 (18 °C) and LA127 (30 °C), by growing them in triplicate 1L polycarbonate bottles for 2 wk at 22 °C with dilutions every three days. After 2 wk, cultures were diluted to equal biomass and the temperature was increased to 28 °C and sampled for POC and carbon fixation (following methods in ref. 58). Sampling was repeated two and four days following the temperature increase.

Differences in photosystem efficiency were also measured for both LA31 and LA127. To detect the instantaneous dissociation temperature of the phycocyanin antenna complex, 200 mL of triplicate cultures was grown at 22 °C to maximum density while still in the exponential growth phase (as determined with fluorescence). They were concentrated by centrifuging for 15 min at  $27,000 \times g$ . Cell pellets were then resuspended in 5 mL of sterile media, and fluorescence was measured on a SpectraMax m2<sup>e</sup> (Molecular Devices) from 600 to 700 nm after excitation at 530 nm (59) every three degrees from 22 to 57 °C (10-min incubation at each temperature) following the methods of ref. 30. The uppertemperature limit used for this photobiology assay is based on the Tmax of the photosystem rather than that of the whole cell. In addition, we measured the photosynthetic efficiency of photosystem II (Fv/Fm) when acclimated to 28 °C using a PHYTO-PAM with an excitation wavelength of 645 nm for C-phycocyanin and allophycocyanin (Heinz Walz). Fv/Fm measurements were made using triplicate cultures, and three technical replicates that were dark acclimated for 20 min (following ref. 60).

DNA Extraction, Sequencing, and Analysis. First, 250 mL of maximum biomass culture for each strain was filtered onto 0.2-µm polyethersulfone membrane filters and DNA was extracted using the DNeasy PowerSoil kit (Qiagen). Then, ~10 million 2 × 150 Illumina Hiseq reads were generated at Novogene Inc. per isolate. Read filtering was done with bbduk (bbmap, v.38.90), and all reads mapped to the available reference genome for LA31 GCF\_018502385.1 (25) using bowtie2 v.2.4.3 (61), and separated from non-Synechococcus reads using samtools v.1.11 (62) and BEDtools v.2.30 (63). Synechococcus reads were normalized to 60× coverage using bbnorm (bbmap, v.38.90) and assembled with SPAdes v.3.15.2 (64).

Relatedness was determined using fastANI v.1.2 (65) to calculate average nucleotide identity (ANI). For comparison, the genome of closely related isolate CB0101 was included (66). All short-read assemblies were aligned to the closed reference genome for LA31 to detect single-nucleotide polymorphisms (SNPs) within the core genome using parsnp v.1.2 and gingr v.1.3 (67). Genes were identified with prodigal v.2.6.3 (68) and annotated using kofamScan v.1.1.0 (69) then imported into the Anvi'o v.7.0 (70) pangenomic pipeline.

In addition, DNA was extracted from low-temperature (18 °C) strain LA31 and high-temperature (30 °C) strain LA127 for long-read sequencing using an Oxford Nanopore Minion with the FLO-MIN106D flow cell. Library prep was done using the Ligation Sequencing Kit (SQK-LSK109) and Rapid Barcoding Kit (SQK-RBK004) following the Genomic DNA by Ligation protocol (https://nanoporetech.com/ automated\_library\_prep\_with\_dreamprep). Then, 200 mL of culture grown to maximum density was concentrated using centrifugation (27,000 × g for 15 min) and extracted with the GenElute Bacterial Genomic DNA Kit (Millipore Sigma). Base-calling was done using guppy v.2.2.3, and long reads were filtered using filtLong v.0.2.0 (https://github.com/rrwick/Filtlong). Filtered reads were mapped to their respective short read assemblies using minimap2 v.2.17 (71). Mapped reads were then assembled along with short-reads using unicycler v.0.4.8 (72). Then, 5-methylcytosine was detected from raw Minion output using nanopolish v.0.13.2 (73). Methylation sites were only considered if they were present in at least 70% of long-reads. Microscopy suggested that these isolate cultures were nonaxenic, but bacteria were a relatively minor component of the microbial biomass. The metaphlan (74) pipeline (v.3.0.8) was used to screen the heterotrophic bacterial community.

Genome Methylation Null Modeling. A null model approach was used to estimate whether observed genome methylation distributions were significantly different from those predicted by chance alone. To first examine whether methylated sites were enriched in coding regions in LA127 and LA31 genomes, each genome's coding sequences were randomly subsampled 1,000 times to create 1,000 sets of randomly sampled genes. Next, for each subsampled coding set in each genome, the number of instances where observed methylated

sites overlapped with each simulated coding set was counted to generate a null distribution. The number of instances where simulated methylated sites within each subsampled coding set were equal to or greater than the instances of observed methylated sites in each genome's coding regions was then counted. To similarly determine potential enrichment of methylation in all photosystem-related genes, the same approach was used, except now the number of instances were counted where methylated sites in photosystem-related genes overlapped with subsampled coding sequences, and statistically compared relative to the observed methylation in photosystem-related coding sequences. Finally, the difference in the several uniquely methylated photosystem-related genes in the two epigenomes from LA127 (2 genes) and LA31 (5 genes) was estimated relative to total photosystem gene methylation enrichment in these genomes, although it should be noted that the comparison was based on only two samples.

Analysis of Long-Term Temperature Trends. In order to explore changes in summertime temperature trends at our study site, all available SST data from 1957 through 2019 collected as part of the long-term times series weekly measurements were downloaded from <a href="https://web.uri.edu/gso/research/plankton/data/">https://web.uri.edu/gso/research/plankton/data/</a>. All measurements from June to August were aggregated by year and a simple linear model used to calculate the rate temperature increase. The slope of this linear model was then used to predict the distribution of summertime temperature in the year 2100. A normal distribution was assumed for both present day and future temperatures, as well as a similar SD from the mean.

**Data, Materials, and Software Availability.** Curated genomes are available from the National Center for Biotechnology Information (75). Isolate information and individual BioSample accession numbers can be found in *SI Appendix*, Table S2. Scripts used in the analysis and generation of all figures as well as

- J. A. Fuhrman, F. Azam, Thymidine incorporation as a measure of heterotrophic bacterioplankton production in marine surface waters: Evaluation and field results. Mar. Biol. 66, 109–120 (1982).
- Rev. Microbiol. 20, 401–414 (2022).

  K. I. Locey, J. T. Lennon, Scaling laws predict global microbial diversity. Proc. Natl. Acad. Sci. U.S.A.

D. A. Hutchins, D. G. Capone, The ocean nitrogen cycle: New developments and global change. Nat.

- K.J. Locey, J.T. Lennon, Scaling laws predict global microbial diversity. Proc. Natl. Acad. Sci. U.S.A. 113, 5970-5975 (2016).
- M. Chafee et al., Recurrent patterns of microdiversity in a temperate coastal marine environment. ISME J. 12, 237–252 (2018).
- D. M. Needham, R. Sachdeva, J. A. Fuhrman, Ecological dynamics and co-occurrence among marine phytoplankton, bacteria and myoviruses shows microdiversity matters. ISME J. 11, 1614–1629 (2017).
- T. O. Delmont et al., Single-amino acid variants reveal evolutionary processes that shape the biogeography of a global SAR11 subclade. Elife 8, e46497 (2019).
- N. Kashtan et al., Single-cell genomics reveals hundreds of coexisting subpopulations in wild Prochlorococcus. Science 344, 416–420 (2014).
- J. A. Sohm et al., Co-occurring Synechococcus ecotypes occupy four major oceanic regimes defined by temperature, macronutrients and iron. ISME J. 10, 333–345 (2016).
- N. García-García, J. Tamames, A. M. Linz, C. Pedrós-Alió, F. Puente-Sánchez, Microdiversity ensures the maintenance of functional microbial communities under changing environmental conditions. ISME J. 13, 2969–2983 (2019).
- A. Shade et al., Fundamentals of microbial community resistance and resilience. Front. Microbiol. 3, 417 (2012).
- M. K. Thomas, C. T. Kremer, C. A. Klausmeier, E. Litchman, A global pattern of thermal adaptation in marine phytoplankton. *Science* 338, 1085–1088 (2012).
- D. A. Hutchins et al., Climate change microbiology-problems and perspectives. Nat. Rev. Microbiol. 17, 391–396 (2019).
- R. Cavicchioli et al., Scientists' warning to humanity: Microorganisms and climate change. Nat. Rev. Microbiol. 17, 569-586 (2019).
- A. E. Zimmerman, S. D. Allison, A. C. Martiny, Phylogenetic constraints on elemental stoichiometry and resource allocation in heterotrophic marine bacteria. *Environ. Microbiol.* 16, 1398–1410 (2014).
- D. A. Hutchins, F.-X. Fu, E. A. Webb, N. Walworth, A. Tagliabue, Taxon-specific response of marine nitrogen fixers to elevated carbon dioxide concentrations. *Nat. Geosci.* 6, 790–795 (2013).
- F. X. Fu et al., Differing responses of marine N2 fixers to warming and consequences for future diazotroph community structure. Aquat. Microb. Ecol. 72, 33–46 (2014).
- N. D. Olson et al., Metagenomic assembly through the lens of validation: Recent advances in assessing and improving the quality of genomes assembled from metagenomes. Brief. Bioinform. 20, 1140–1150 (2019).
- 18. D. A. Hutchins, F. Fu, Microorganisms and ocean global change. Nat. Microbiol. 2, 17058 (2017).
- J. D. Kling et al., Transient exposure to novel high temperatures reshapes coastal phytoplankton communities. ISME J. 14, 413-424 (2020).
- R. K. Pachauri et al., "Climate Change 2014: Synthesis Report. Contribution of Working Groups I, II, and III to the Fifth Assessment Report of the Intergovernmental Panel on Climate Change", R. K. Pachauri, L. Meyer, Eds. (IPCC, Geneva, Switzerland, 2014), pp. 151.
- M. D. Lee et al., Marine Synechococcus isolates representing globally abundant genomic lineages demonstrate a unique evolutionary path of genome reduction without a decrease in GC content. Environ. Microbiol. 21, 1677–1686 (2019).

all physiological data are available on github (76). Phenotypic data are also available at the Biological and Chemical Oceanography Data Management Office (77–79).

ACKNOWLEDGMENTS. This work was funded by US NSF Dimensions of Biodiversity grants OCE1638804 to D.A.H., OCE1638834 to T.A.R., and OCE1638958 to E.L., and by OCE1851222 to D.A.H. and E.A.W. and OCE 2149837 to D.A.H. This study is based on work conducted at the URI Marine Science Research Facility supported in part by the NSF EPSCoR awards OIA-1004057 and OIA-1655221. Illumina sequencing was supported by the Global Climate Change and Ocean Atmosphere Interaction Project, Marine Biological Sample Museum Upgrade and Expansion Project (GASI-01-02-04) to Q.Z. and C.W. Thanks to David Kehoe (Indiana University) for helpful insights into *Synechococcus* photophysiology and to J. Cameron Thrash (University of Southern California) and Ben Temperton (University of Exeter) for helping generate and perform base calling on Minion long reads.

Author affiliations: <sup>a</sup>Department of Biological Sciences, University of Southern California, Los Angeles, CA 90007; <sup>b</sup>ZOLL Medical Corporation, Chelmsford, MA 01824; <sup>c</sup>Blue Marble Space Institute of Science, Seattle, WA 98154; <sup>d</sup>Kellogg Biological Station, College of Natural Science, Michigan State University, Hickory Corners, MI 49060; <sup>c</sup>Graduate School of Oceanography, The University of Rhode Island, Narragansett, RI 02882; <sup>d</sup>Department of Earth, Atmospheric and Planetary Sciences, Massachusetts Institute of Technology, Cambridge, MA 02139; <sup>a</sup>Third Institute of Oceanography, Ministry of Natural Resources, Xiamen, Fujian 361005, China; <sup>b</sup>Department of Ecology and Evolutionary Biology, University of Connecticut, Storrs, CT 06269; and <sup>b</sup>Department of Global Ecology, Carnegie Institution, Stanford University, Palo Alto, CA 94305

Author contributions: J.D.K. and D.A.H. designed research; J.D.K., N.G.W., J.T.C., P.W., S.I.A., Q.Z., M.D.P., F.F., C.T.K., E.L., and T.A.R. performed research; C.W. contributed new reagents/analytic tools; J.D.K., M.D.L., N.G.W., E.A.W., P.W., S.I.A., Q.Z., F.F., T.A.R., and D.A.H. analyzed data; and J.D.K., M.D.L., N.G.W., E.A.W., J.T.C., P.W., S.I.A., Q.Z., C.W., M.D.P., F.F., C.T.K., E.L., T.A.R., and D.A.H. wrote the paper.

- P. Flombaum et al., Present and future global distributions of the marine Cyanobacteria Prochlorococcus and Synechococcus. Proc. Natl. Acad. Sci. U.S.A. 110, 9824–9829 (2013).
- S. I. Anderson, A. D. Barton, S. Clayton, S. Dutkiewicz, T. A. Rynearson, Marine phytoplankton functional types exhibit diverse responses to thermal change. *Nat. Commun.* 12, 6413 (2021).
- L. Guidi et al., Plankton networks driving carbon export in the oligotrophic ocean. Nature 532, 465–470 (2016).
- J. D. Kling, E. A. Webb, D. A. Hutchins, Genome sequence of Synechococcus sp. strain LA31, isolated from a temperate estuary. Microbiol. Resour. Announc. 11, e0077521 (2022).
- N. G. Walworth et al., Long-term m5C methylome dynamics parallel phenotypic adaptation in the cyanobacterium Trichodesmium. Mol. Biol. Evol. 38, 927–939 (2021).
- J. P. Zehr, K. Ohki, Y. Fujita, D. Landry, Unique modification of adenine in genomic DNA of the marine cyanobacterium *Trichodesmium* sp. strain NIBB 1067. J. Bacteriol. 173, 7059-7062 (1991).
- J. E. Barrick, R. E. Lenski, Genome dynamics during experimental evolution. Nat. Rev. Genet. 14, 827–839 (2013).
- S. F. Elena, R. E. Lenski, Microbial genetics: Evolution experiments with microorganisms: The dynamics and genetic bases of adaptation. *Nat. Rev. Genet.* 4, 457–469 (2003).
- J. Pittera, F. Partensky, C. Six, Adaptive thermostability of light-harvesting complexes in marine picocyanobacteria. ISME J. 11, 112–124 (2017).
- A. W. Thompson, K. Kouba, Differential activity of coexisting *Prochlorococcus* ecotypes. Front. Marine Sci. 6, 701 (2019), 10.3389/fmars.2019.00701.
- J. Pittera et al., Connecting thermal physiology and latitudinal niche partitioning in marine Synechococcus. ISME J. 8, 1221–1236 (2014).
- T. Grébert et al., Light color acclimation is a key process in the global ocean distribution of Synechococcus cyanobacteria. Proc. Natl. Acad. Sci. U.S.A. 115, E2010-E2019 (2018).
- K. R. M. Mackey et al., Effect of temperature on photosynthesis and growth in marine Synechococcus spp. Plant Physiol. 163, 815–829 (2013).
- H. Innan, F. Kondrashov, The evolution of gene duplications: Classifying and distinguishing between models. Nat. Rev. Genet. 11, 97–108 (2010).
- J. H. Costello, B. K. Sullivan, D. J. Gifford, D. Van Keuren, L. J. Sullivan, Seasonal refugia, shoreward thermal amplification, and metapopulation dynamics of the ctenophore *Mnemiopsis leidyiin* Narragansett Bay, Rhode Island. *Limnol. Oceanogr.* 51, 1819–1831 (2006).
- M. A. Doblin, E. van Sebille, Drift in ocean currents impacts intergenerational microbial exposure to temperature. Proc. Natl. Acad. Sci. U.S.A. 113, 5700–5705 (2016).
- C. Kincaid, Spatial and temporal variability in flow at the mouth of Narragansett Bay. J. Geophys. Res. 108, C7 (2003), 10.1029/2002JC001395.
- D. G. Borkman, T. J. Smayda, Gulf stream position and winter NAO as drivers of long-term variations in the bloom phenology of the diatom Skeletonema costatum "species-complex" in Narragansett Bay, RI, USA. J. Plankton Res. 31, 1407–1425 (2009).
- K. L. Canesi, T. A. Rynearson, Temporal variation of Skeletonema community composition from a long-term time series in Narragansett Bay identified using high-throughput DNA sequencing. Mar. Ecol. Prog. Ser. 556, 1–16 (2016), 10.3354/meps11843.
- A. J. M. Wood, J. S. Collie, J. A. Hare, A comparison between warm-water fish assemblages of Narragansett Bay and those of Long Island Sound waters. Fish. Bull. 107, 89–100 (2009).
- E. Schaum, B. Rost, A. J. Millar, S. Collins, Variation in plastic responses of a globally distributed picoplankton species to ocean acidification. *Nat. Clim. Chang.* 3, 298–302 (2012).

- S. I. Anderson, T. A. Rynearson, Variability approaching the thermal limits can drive diatom community dynamics. *Limnol. Oceanogr.* 65, 1961–1973 (2020).
- M. Hagemann et al., Identification of the DNA methyltransferases establishing the methylome of the cyanobacterium Synechocystis sp. in PCC 6803. DNA Res. 25, 343–352 (2018).
- K. Gärtner et al., Cytosine N4-methylation via M.Ssp6803II is involved in the regulation of transcription, fine- tuning of DNA replication and DNA repair in the Cyanobacterium Synechocystis sp. PCC 6803. Front. Microbiol. 10, 1233 (2019).
- M. A. Sánchez-Romero, I. Cota, J. Casadesús, DNA methylation in bacteria: From the methyl group to the methylome. Curr. Opin. Microbiol. 25, 9–16 (2015).
- H. J. Seong, S.-W. Han, W. J. Sul, Prokaryotic DNA methylation and its functional roles. J. Microbiol. 59, 242–248 (2021).
- 48. K. Bräutigam *et al.*, Épigenetic regulation of adaptive responses of forest tree species to the environment. *Ecol. Evol.* **3**, 399-415 (2013).
- J. Pazzaglia et al., DNA methylation dynamics in a coastal foundation seagrass species under abiotic stressors. Proc. Biol. Sci. 290, 20222197 (2023).
- V. Douhovnikoff, R. S. Dodd, Epigenetics: A potential mechanism for clonal plant success. *Plant Ecol.* 216, 227–233 (2015).
- A. Tourancheau, E. A. Mead, X.-S. Zhang, G. Fang, Discovering multiple types of DNA methylation from bacteria and microbiome using nanopore sequencing. Nat. Methods 18, 491–498 (2021).
- H. J. Seong, S. Roux, C. Y. Hwang, W. J. Sul, Marine DNA methylation patterns are associated with microbial community composition and inform virus-host dynamics. *Microbiome* 10, 157 (2022).
- R. R. L. Guillard, "Culture of phytoplankton for feeding marine invertebrates" in Culture of Marine Invertebrate Animals: Proceedings – 1st Conference on Culture of Marine Invertebrate Animals Greenport, W. L. Smith, M. H. Chanley, Eds. (Springer, US, 1975), pp. 29–60.
- W. G. Sunda, N. M. Price, F. M. M. Morel, "Trace metal ion buffers and their use in culture studies" in Algal Culturing Techniques (Academic Press, Burlington, MA, USA, 2005).
- T. A. Rynearson, S. A. Flickinger, D. N. Fontaine, Metabarcoding reveals temporal patterns of community composition and realized thermal niches of *Thalassiosira spp*. (Bacillariophyceae) from the Narragansett Bay long-term plankton time series. *Biology* 9, 19 (2020).
- J. Norberg, Biodiversity and ecosystem functioning: A complex adaptive systems approach. Limnol. Oceanogr. 49, 1269–1277 (2004).
- R. C. Team et al., R: A language and environment for statistical computing (Version 3.0.0, R Foundation for Statistical Computing, Vienna, Austria, 2013).
- P. Qu, F. Fu, D. A. Hutchins, Responses of the large centric diatom Coscinodiscus sp. to interactions between warming, elevated CO<sub>2</sub>, and nitrate availability. Limnol. Oceanogr. 63, 1407–1424 (2018).
- C. Six et al., Two novel phycoerythrin-associated linker proteins in the marine cyanobacterium Synechococcus sp. strain WH8102. J. Bacteriol. 187, 1685–1694 (2005).
- E. L. McParland, A. Wright, K. Art, M. He, N. M. Levine, Evidence for contrasting roles of dimethylsulfoniopropionate production in *Emiliania huxleyi* and *Thalassiosira oceanica*. New Phytol. 226, 396–409 (2020).

- B. Langmead, S. L. Salzberg, Fast gapped-read alignment with Bowtie 2. Nat. Methods 9, 357–359 (2012)
- P. Danecek et al., Twelve years of SAMtools and BCFtools. Gigascience 10, giab008 (2021), 10.1093/ gigascience/giab008.
- Ä. R. Quinlan, I. M. Hall, BEDTools: A flexible suite of utilities for comparing genomic features. Bioinformatics 26, 841–842 (2010).
- A. Bankevich et al., SPAdes: A new genome assembly algorithm and its applications to single-cell sequencing. J. Comput. Biol. 19, 455-477 (2012).
- C. Jain, L. M. Rodriguez-R, A. M. Phillippy, K. T. Konstantinidis, S. Aluru, High throughput ANI analysis of 90K prokaryotic genomes reveals clear species boundaries. *Nat. Commun.* 9, 5114 (2018).
- D. Marsan, K. E. Wommack, J. Ravel, F. Chen, Draft denome sequence of *Synechococcus* sp. strain CB0101, isolated from the Chesapeake bay estuary. *Genome Announc.* 2, e01111-13 (2014).
- T. J. Treangen, B. D. Ondov, S. Koren, A. M. Phillippy, The Harvest suite for rapid core-genome alignment and visualization of thousands of intraspecific microbial genomes. *Genome Biol.* 15, 524 (2014).
- D. Hyatt et al., Prodigal: Prokaryotic gene recognition and translation initiation site identification BMC Bioinform. 11, 119 (2010).
- T. Aramaki et al., KofamKOALA: KEGG Ortholog assignment based on profile HMM and adaptive score threshold. Bioinformatics 36, 2251–2252 (2020).
- 70. A. M. Eren *et al.*, Anvi/o: An advanced analysis and visualization platform for 'omics data. *PeerJ* 3,
- e1319 (2015).
  71. H. Li, Minimap 2: Pairwise alignment for nucleotide sequences. *Bioinformatics* **34**, 3094–3100
- (2018).
  72. R. R. Wick, L. M. Judd, C. L. Gorrie, K. E. Holt, Unicycler: Resolving bacterial genome assemblies from
- short and long sequencing reads. *PLoS Comput. Biol.* **13**, e1005595 (2017).

  73. J. T. Simpson *et al.*, Detecting DNA cytosine methylation using nanopore sequencing. *Nat. Methods* **14**, 407–410 (2017).
- F. Beghini et al., Integrating taxonomic, functional, and strain-level profiling of diverse microbial communities with bioBakery 3. Elife 10, e65088 (2021).
- J. D. Kling, Intraspecific variation of thermal niche in coastal Synechococcus. National Center for Biotechnology Information BioProject. https://www.ncbi.nlm.nih.gov/ bioproject/?term=PRJNA566206. Deposited 18 September 2019.
- J. D. Kling, JDKling/Syn\_microdiversity. Github. https://github.com/JDKling/Syn\_microdiversity. Deposited 18 August 2021.
- J. D. Kling, Dataset: Synechococcus fluorescence emission spectra. Biological and Chemical Oceanography Data Management Office. https://www.bco-dmo.org/dataset/782322. Deposited 20 November 2019.
- J. D. Kling, Dataset: Synechococcus growth rates. Biological and Chemical Oceanography Data Management Office. https://www.bco-dmo.org/dataset/782314. Deposited 20 November 2019.
- J. D. Kling, Dataset: Synechococcus TPC parameters. Biological and Chemical Oceanography Data Management Office. https://www.bco-dmo.org/dataset/782308. Deposited 20 November 2019.